

## Preparation and Photoelectronic Properties of the System $\text{Cd}_2\text{Ge}_{1-x}\text{Si}_x\text{O}_4$

VAN SON NGUYEN, ROBERT KERSHAW, KIRBY DWIGHT, AND AARON WOLD\*

*Department of Chemistry, Brown University, Providence, Rhode Island 02912*

Received May 6, 1980; in final form July 28, 1980

Members of the system  $\text{Cd}_2\text{Ge}_{1-x}\text{Si}_x\text{O}_4$  where  $0 \leq x \leq 0.4$  have been prepared. These compounds were observed to crystallize with the olivine structure, space group *Pbnm*. The resistivity, Hall mobility, flat-band potential, band gaps, and stability were determined as functions of composition. The variation of these photoelectronic properties can be attributed to the reduction of the cell parameters with increasing silicon substitution. The substitution of silicon for germanium reduces the loss of photocurrent from 25% after 1 hr for  $x = 0.0$  to only 6% after 22 hr for  $x = 0.4$ .

### Introduction

There have been several excellent review papers which have summarized recent investigations concerning the photoelectrolysis of water using *n*-type semiconducting transition metal oxides (1, 2). The oxides  $\text{TiO}_{2-x}$  and  $\text{WO}_{3-x}$  (3,4) were shown to have low electron mobilities ( $\leq 0.1 \text{ cm}^2/\text{V} \cdot \text{sec}$ ) and high carrier concentrations ( $\sim 10^{19}/\text{cm}^3$ ). The conductivity of other metal oxides, e.g., antimony-doped tin (IV) oxide (5), is due to fewer carriers ( $\sim 10^{18}/\text{cm}^3$ ) with high mobility ( $\sim 20 \text{ cm}^2/\text{Y} \cdot \text{sec}$ ).

Another example of an oxide which has a high mobility is  $\text{Cd}_2\text{GeO}_4$  (6). This compound is more stable as an electrode in aqueous solution than  $\text{Cd}_2\text{SnO}_4$  (7). Since the stability is increased by the substitution of germanium for tin, it may be possible to further increase the stability of the elec-

trode in aqueous solution by the preparation of photoanodes from members of the series  $\text{Cd}_2\text{Ge}_{1-x}\text{Si}_x\text{O}_4$ . In addition, the effect of such substitution on the flat-band potential and band gap can also be determined.

### Synthesis and Experimental Techniques

Samples of  $\text{Cd}_2\text{Ge}_{1-x}\text{Si}_x\text{O}_4$  ( $x = 0.0, 0.2, 0.4$ ) were prepared by the solid-state reaction of appropriate quantities of  $\text{GeO}_2$  (Johnson Matthey, spec. pure),  $\text{CdO}$  (obtained from the decomposition of  $\text{CdCO}_3$ ), and  $\text{SiO}_2$  (obtained by the hydrolysis of  $\text{SiCl}_4$ ). Cadmium carbonate was subjected to thermogravimetric analysis; the weight of cadmium oxide obtained from the thermal decomposition of cadmium carbonate at  $320^\circ\text{C}$  agreed with the calculated value. No further weight loss occurred until  $825^\circ\text{C}$ ; however, there was an observable loss in weight of the sample when the

\* To whom all correspondence should be addressed.

temperature exceeded 825°C, indicating volatilization of CdO. As a result of this study, the reaction temperature for the formation of the cadmium compounds is maintained below 825°C in order to prevent loss of CdO. The silicon dioxide was obtained by the hydrolysis of silicon(IV) chloride with the formation of silica gel which was then heated at 800°C for 48 hr, under vacuum, in order to remove all of the water.

Finely ground mixtures of appropriate amounts of each starting material were heated in evacuated silica tubes at 800°C. The samples were removed from the furnace and reground thoroughly twice during the heat treatment, which was carried out for a total of 144 hr. Completed reactions were confirmed by X-ray analysis using a Philips Norelco diffractometer with  $CuK\alpha$  radiation ( $\lambda = 1.5405 \text{ \AA}$ ) and at a scan rate of  $0.25^\circ 2\theta \text{ min}^{-1}$ .

Disks of each composition were prepared by pressing aliquots of approximately 200 mg of the product at 60,000 psi and then heating the green disks in evacuated silica tubes at 800°C for 72 hr. Well-sintered disks, off-white in color, were obtained by this method despite the low sintering temperature necessitated by the possible loss of CdO above 825°C.

### Photoelectronic Properties

Seebeck and D. C. Hall measurements showed all of the compounds to be *n*-type semiconductors; the carrier concentrations (*n*), mobilities ( $\mu$ ), and resistivities ( $\rho$ ) of each compound are reported in Table I. Resistivity measurements were made on representative disks of each composition using the van der Pauw method (8). Indium electrical contacts were applied to each disk by ultrasonic soldering, and ohmic behavior was verified. The thermal variation of resistivity yields an activation energy of 0.017(2) eV for  $Cd_2Ge_{1-x}Si_xO_4$  ( $x = 0.0, 0.2, 0.4$ ).

Photoanodes were prepared by evaporating thin films of gold onto the backs of the disks in order to provide good electrical contact. Anode assemblies were fabricated by first using indium metal to solder these electrodes to platinum wires which had been sealed in small Pyrex tubes, and then coating all but the front surface with an electrically insulating resin (Microstop, Michigan Chrome and Chemical Co.). Care was taken not to disturb the photoactive surfaces. For photoresponse measurements, these anodes were mounted in a small glass cell described previously (9).

TABLE I  
 $Cd_2Ge_{1-x}Si_xO_4$

$n_x$	Si <sub>0.0</sub>	Si <sub>0.2</sub>	Si <sub>0.4</sub>
<i>a</i> (Å)	5.20(1)	5.18(1)	5.15(1)
<i>b</i> (Å)	11.14(1)	11.13(1)	11.10(1)
<i>c</i> (Å)	6.57(1)	6.57(1)	6.55(1)
Resistivity ( $\Omega\text{-cm}$ ) R.T.	0.20(2)	0.60(5)	1.60(5)
Carrier concentration ( $\text{cm}^{-3}$ )	$1.05(5) \times 10^{18}$	$5.1(2) \times 10^{17}$	$2.85(5) \times 10^{17}$
Mobility ( $\text{cm}^2/\text{V} \cdot \text{sec}$ )	30(3)	21(2)	14.0(2)
Flat-band potential (V vs SCE at pH = 13)	-0.82(5)	-0.89(5)	-0.99(5)
Indirect band gap (eV)	3.04(5)	3.20(2)	3.30(2)
Direct band gap (eV)	4.15(5)	4.20(5)	4.45(5)
$I/I_0$ after 1 hr	0.75	0.90	0.95
$I/I_0$ after 5 hr	0.65	0.88	0.91

The anode was placed in 8 mm behind the quartz window. A platinized platinum cathode ( $2.5 \text{ cm}^2$  in area) was mounted 2 cm behind and below the anode and a saturated calomel reference electrode (SCE) above it. The cell was filled with 100 ml of 0.2 M sodium acetate solution which was adjusted to a pH of 13 by the addition of sodium hydroxide. This electrolyte was purged of dissolved oxygen and stirred by means of a continuous stream of 85% argon–15% hydrogen gas. A cathode potential of approximately  $-0.99 \text{ V}$  vs SCE was achieved and used as an indication of complete purging of the cell (9).

A quartz lens was used to focus the light from a 150-W Xenon arc onto an area of 2.25 mm in diameter, and a 1.0 neutral density filter (Oriol Optic Corp.) was used to reduce the irradiation to approximately 40 mW of total power. A monochromator (Oriol Model 7240) with 1-mm slits was used for the spectral studies, and a calibrated silicon photodiode (United Detector Technology) was used to measure the light flux incident on the cell. Anodic bias was applied via a voltage follower having an output impedance of less than  $0.1 \Omega$  and the resulting photoresponse was measured with a current amplifier which inserted a negligible potential drop (less than  $1 \mu\text{V}$ ) into the external circuit.

## Results and Discussion

Tarte (10) reported that  $\text{Cd}_2\text{GeO}_4$  crystallizes with the olivine structure, space group  $Pbnm$ . In this structure, independent  $\text{GeO}_4$  tetrahedra are linked to  $\text{CdO}_6$  octahedra by sharing corners and edges. Two crystallographically independent Cd atoms are both octahedrally surrounded by six oxygens; these octahedra share edges and corners with both  $\text{GeO}_4$  tetrahedra and adjacent octahedra. The oxygen atoms form a slightly distorted hexagonal close-packed array with the hexagonal axis in the  $a$

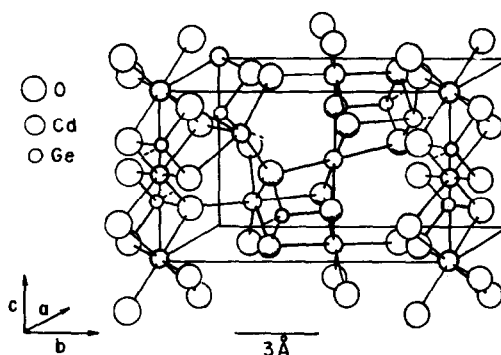


FIG. 1. The olivine structure  $\text{Cd}_2\text{GeO}_4$ .

direction. The cations occupy some of the tetrahedral and octahedral interstices. This structure is shown in Fig. 1. A complete discussion of the olivine structure has been reported by Hanke (11).

$\text{Cd}_2\text{SiO}_4$  crystallizes with the  $[\text{Na}_2\text{SO}_4\text{V}]$  structure (room-temperature form of  $\text{Na}_2\text{SO}_4$ , space group  $Fddd$ ). The structure consists of nearly regular and isolated  $\text{SiO}_4$  tetrahedra, which are held together by irregular  $\text{CdO}_6$  octahedra with each  $\text{SiO}_4$  tetrahedra sharing two opposite edges with two  $\text{CdO}_6$  octahedra (12).  $\text{Cd}_2\text{SnO}_4$  crystallizes with the  $[\text{Sr}_2\text{PbO}_4]$  structure, space group  $Pbam$ . In this structure the edge-shared  $\text{SnO}_6$  octahedra extend in chains in the  $c$  direction. These chains are held together by  $\text{CdO}_7$  polyhedra (13).

The X-ray diffraction patterns for  $\text{Cd}_2\text{Ge}_{1-x}\text{Si}_x\text{O}_4$  ( $x = 0.0, 0.2, 0.4$ ) indicate that these compounds retain the olivine structure. Table I summarizes the crystallographic data for members of the system which were prepared as single phases and studied. Attempts to prepare compounds where  $x > 0.4$  gave multiphase products.

The variations of photoresponse with anode potential obtained for the different samples prepared above are shown in Fig. 2. The values for the flat-band potentials (relative to SCE) given in Table I were consistently determined from extrapolation of the photocurrent, as shown in Fig. 2. Although

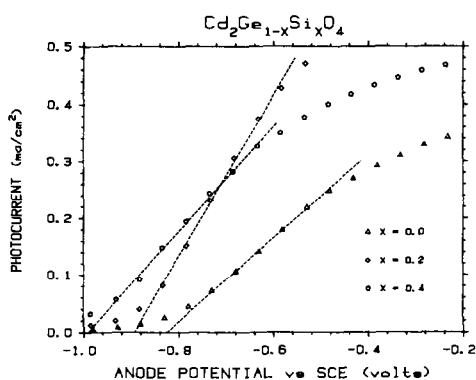


FIG. 2. Photoresponse under "white" xenon arc irradiation of  $1.0 \text{ W/cm}^2$  in  $\text{pH} \approx 13$  electrolyte.

there may be some uncertainty in each of these values, nevertheless, the existence of a progressive change with composition is evident.

The quantum efficiency (photocurrent divided by incident light flux) was measured as a function of wavelength for these samples. This quantum efficiency  $\eta$  is proportional to the optical absorption coefficient  $\alpha$  under the conditions of the experiment (4). Consequently, the standard graphical analysis of  $\alpha$  by which interband transitions are characterized can be applied with  $\alpha$  replaced by  $\eta$ . Accordingly, the quantity  $(\eta h\nu)^{0.5}$  is plotted against photon energy  $h\nu$  in Fig. 3. The low-energy portion of such curves should be a straight line if the transition is indirect in character, and the energy intercept gives the value of the band gap.

The lowest-energy data shown in Fig. 3 come from such low quantum efficiencies that they are attributed to band tails. The low-energy transitions are identified as indirect by the fitted straight lines, which yield the band gaps 3.04, 3.20, and 3.30 eV given in Table I for  $x = 0.0, 0.2,$  and  $0.4,$  respectively. The values given in Table I for a high-energy direct band gap in the neighborhood of 4.2 eV were obtained from a similar analysis with the data replotted as  $(\eta h\nu)^2$  against photon energy.

The variation of relative photocurrent with time is shown in Fig. 4. The olivine  $\text{Cd}_2\text{GeO}_4$  is considerably more stable than  $\text{Cd}_2\text{SnO}_4$ , which loses 25% of its photocurrent during the first minute (7), and a further pronounced increase in stability is obtained from the substitution of silicon for germanium in  $\text{Cd}_2\text{Ge}_{1-x}\text{Si}_x\text{O}_4$ . The unsubstituted material loses 25% of its output during the first hour and 35% during the first 5 hr, compared with 5 and 9%, respectively, for  $\text{Cd}_2\text{Ge}_{0.6}\text{Si}_{0.4}\text{O}_4$ . Although off scale in Fig. 4, the data for  $\text{Cd}_2\text{Ge}_{0.6}\text{Si}_{0.4}\text{O}_4$  extends for an additional 15 hr and suffers a further decrease of only 1%.

From the above, it appears that stabilization is obtained by the substitution of tetrahedral silicon(IV) ( $0.26 \text{ \AA}$ ) for tetrahedral germanium(IV) ( $0.39 \text{ \AA}$ ). The results of X-ray analysis and the preference of silicon(IV) for tetrahedral sites establish that the series  $\text{Cd}_2\text{Ge}_{1-x}\text{Si}_x\text{O}_4$  ( $0 \leq x \leq 0.4$ ) all possess the same olivine structure. It would not be unreasonable to attribute an increase in stability to the strengthening of bonds arising from the decrease in cell parameters given in Table I. This strengthening can also increase the band gap and decrease the flat-band potential, as observed.

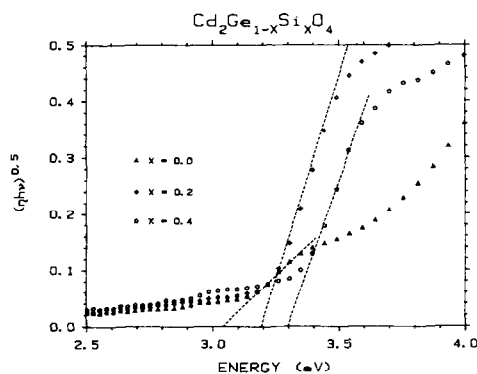


FIG. 3. Band gap determination based on the quantum efficiency measured at an anode potential of  $-0.2 \text{ V vs SCE}$  in  $\text{pH} \approx 13$  electrolyte.

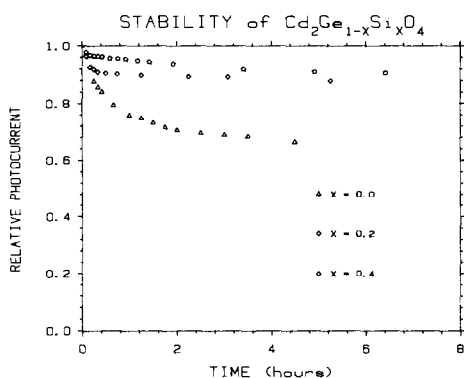


FIG. 4. Stability under "white" xenon arc irradiation of  $1.0 \text{ W/cm}^2$  in  $0.2 \text{ M}$  sodium acetate adjusted to  $\text{pH} \approx 13$ .

### Summary and Conclusion

Single-phase samples of  $\text{Cd}_2\text{Ge}_{1-x}\text{Si}_x\text{O}_4$  ( $x = 0.0, 0.2, 0.4$ ) were prepared from  $\text{CdO}$ ,  $\text{SiO}_2$ , and  $\text{GeO}_2$  which, in turn, were carefully prepared so as to ensure the greatest possible degree of stoichiometry. It was determined that  $\text{CdO}$  loses weight above  $825^\circ\text{C}$ , and consequently all reactions and sinterings were carried out at  $800^\circ\text{C}$ . X-Ray analysis showed all the samples to possess the olivine structure, the cell parameters decreasing with increasing substitution of silicon for germanium.

Measurements were made of the resistivity, Hall effect, and such photoelectronic properties as the current-voltage response, spectral response, and stability. The results listed in Table I follow a systematic variation with composition.

Silicon prefers tetrahedral coordination and its substitution for germanium in  $\text{Cd}_2\text{Ge}_{1-x}\text{Si}_x\text{O}_4$  presents no anomalies. The variation of the observed properties with composition for this system can be attributed to the decrease in cell dimensions, which may increase the strength of chemical bonding. The observed increase in sta-

bility is dramatic; from a 25% loss after 1 hr for  $x = 0.0$  to only a 6% loss after 22 hr for  $x = 0.4$ .

$\text{Cd}_2\text{GeO}_4$  maintains the olivine structure for substitution of up to 40 atom% silicon for germanium. It is the first reported oxide system where such substitutions can modify the fundamental photoelectronic properties of flat-band potential, band gap, and stability.

### Acknowledgments

The authors would like to acknowledge the support of the Office of Naval Research, Arlington, Virginia, for the support of Van Son Nguyen and Kirby Dwight. The authors would also like to acknowledge the Solar Energy Research Institute, Golden, Colorado, as well as the Materials Research Laboratory Program at Brown University for their support.

### References

1. A. J. NOZIK, *Annu. Rev. Phys. Chem.* **29**, 189 (1978).
2. L. A. HARRIS AND R. H. WILSON, *Annu. Rev. Mater. Sci.* **8**, 99 (1978).
3. H. P. R. FREDERIKSE, *J. Appl. Phys.* **32**, 2211 (1961).
4. F. P. KOFFYBERG, K. DWIGHT, AND A. WOLD, *Solid State Commun.* **30**, 433 (1979).
5. C. G. FONSTAD, A. LINZAND, AND R. H. REDIKER, *J. Electrochem. Soc.* **116**, 9, 1269 (1969).
6. V. S. NGUYEN, S. N. SUBBARAO, R. KERSHAW, K. DWIGHT, AND A. WOLD, *Mater. Res. Bull.* **11**, 1535 (1979).
7. V. S. NGUYEN, unpublished results.
8. L. T. VAN DER PAUW, *Philips Tech. Rev.* **20**, 220 (1958).
9. S. N. SUBBARAO, Y. H. YUN, R. KERSHAW, K. DWIGHT, AND A. WOLD, *Inorg. Chem.* **18**, 1488 (1979).
10. P. TARTE, *J. Inorg. Nucl. Chem.* **27**, 1933 (1965).
11. K. HANKE, *Beitr. Mineral. Petrogr.* **11**, 535 (1965).
12. W. H. ZACHARESEN AND G. E. ZIEGLER, *Z. Kristallogr.* **81**, 92 (1932).
13. M. TROMEL, *Z. Anorg. Allg. Chem.* **371**, 237 (1969).